Overexpression of miR-130a-3p/301a-3p attenuates high glucose-induced MPC5 podocyte dysfunction through suppression of TNF-α signaling

YAN JIANG[1*], WEI WANG[2*], ZONG-YANG LIU[1], YI XIE[1], YUAN QIAN[1] and XUE-NI CAI[1]

[1]Department of Nephrology, The Cancer Hospital of Guizhou, Guiyang, Guizhou 550003; [2]Department of Nephrology, The 455 Hospital of Chinese PLA, Nephrology Center of Nanjing Military Area Command of Chinese PLA, Shanghai 200052, P.R. China

Received July 26, 2017; Accepted November 6, 2017

DOI: 10.3892/etm.2017.5465

Abstract. Tumor necrosis factor (TNF)-α has been reported to be important in glomerulonephritis, which is closely associated with podocyte dysfunction and apoptosis. However, the precise mechanisms by which TNF-α expression are regulated remain unclear. The purpose of the present study was to investigate the role of microRNA (miR)-130a-3p/301a-3p in the post-transcriptional control of TNF-α expression and high glucose (HG)-induced podocyte dysfunction. Mice MPC5 podocytes were incubated with HG and transfected with miR-130a-3p/301a-3p mimics or inhibitors, reactive oxygen species (ROS) levels were measured by flow cytometry assay, and the mRNA and protein levels were assayed by using reverse transcription-quantitative polymerase chain reaction and western blotting, respectively. The targeted genes were predicted by a bioinformatics algorithm and verified using a dual luciferase reporter assay. It was observed that miR-130a-3p/301a-3p was a novel regulator of TNF-α in mouse podocytes. miR-130a-3p/301a-3p mimics inhibited TNF-α 3'-untranslated region luciferase reporter activity, in addition to endogenous TNF-α protein expression. Furthermore, forced expression of miR-130a-3p or miR-301a-3p resulted in the downregulation of ROS and malondialdehyde (MDA) and the upregulation of superoxide dismutase (SOD) 1 in the presence of HG. Inhibition of TNF-α level prevented a remarkable reduction in SOD activity and a marked increase in ROS and MDA levels in HG-treated podocytes. Furthermore, TNF-α loss-of-function significantly reversed HG-induced podocyte apoptosis. These data demonstrated a novel up-stream role for miR-130a-3p/301a-3p in TNF-α-mediated podocyte dysfunction and apoptosis in the presence of HG.

Correspondence to: Dr Zong-Yang Liu, Department of Nephrology, The Cancer Hospital of Guizhou, 1 Western Beijing Road, Guiyang, Guizhou 550003, P.R. China
E-mail: liu_zyyh@163.com

*Contributed equally

Key words: miR-130a-3p, miR-301a-3p, podocytes dysfunction, TNF-α, glomerulonephritis

Introduction

Glomerular podocytes are highly differentiated cells that play a key role in maintaining the integrity of the glomerular filtration barrier (1). In glomerular diseases, podocyte damage leads to increased glomerular barrier pore size, allowing the passage of proteins or other mediators to the tubular lumen, which results in proteinuria and progressive loss of kidney function (2). Accumulating evidence indicates that hyperglycemia contributes to podocyte lesions (3). Clinical data demonstrate that podocyte integrity is impaired, and the decreased podocyte number is confirmed in individuals with type 1 (T1DM) and 2 diabetes mellitus (T2DM) (4,5). In cultured podocytes, high glucose induces apoptosis, epithelial-mesenchymal transition (EMT), mitochondrial fission and autophagy through different signaling pathways (6-9). However, the underlying molecular mechanisms of high glucose-induced MPC5 podocytes dysfunction remain to be fully elucidated.

MicroRNAs (miRs) are endogenous, noncoding, short, single-stranded RNAs (18-25 nucleotides) that are evolutionarily highly conserved, believed to regulate the translation of target messenger RNAs (mRNAs) by binding to its 3'-untranslated regions (3'-UTRs) and verified to play a role in controlling a variety of biological processes (10). Recently, several studies have highlighted the significance of miRs in maintaining glucose metabolism-associated cell dysfunction (11-13). For example, miR-130a-3p has been shown to mediate insulin sensitivity (10), and miR-24-3p, miR-146a-5p, miR-194-5p, miR-197-3p, miR-301a-3p and miR-375 are correlated with residual beta cell function in children with new-onset type 1 diabetes mellitus (T1DM) (12). Moreover, miR-27a, miR-34a, miR-195 and miR-218 promote podocyte injury (6,14-16), in contrast to that miR-29a, miR-30a and miR-217 protect against high glucose-induced podocyte injury (9,17,18). These findings suggest that the regulation of these miRs may serve as potential therapeutic targets in high glucose-induced cell dysfunction.

miR-130a-3p and miR-301a-3p belong to miR-130 and miR-301 family individually, which are mainly identified in

mouse (19,20). miR-130a has been deemed a glucose-regulated miR, and miR-130a expression is significantly down-regulated by high glucose at 16.7 mM in pancreatic islets compared with control group (21). Moreover, miR-301a is involved in hyperglycemia-induced cardiac injury (13). These results suggest that miR-130a-3p and miR-301a-3p play a critical role in diabetes-related complications. However, there has been no relevant report about the post-transcriptional mechanism of miR-130a-3p/301a-3p in high glucose-induced podocytes dysfunction. In the present study, utilizing on-line prediction algorithms, we had identified that miR-130a-3p and miR-301a-3p shared the same seed site sequence of TNF gene. *In vitro* study on the MPC5 podocytes was designed to experimentally validate the targeting relationship between miR-130a-3p/301a-3p and TNF-α in high glucose-mediated podocytes dysfunction.

Materials and methods

Cell culture. Conditionally immortalized mouse podocytes (MPC5) were obtained from Dr Peter MUNDEL (Mount Sinai School of Medicine, New York, USA) and maintained in RPMI-1640 (Invitrogen, Carlsbad, CA, USA) supplemented with 10% FBS (Invitrogen) at 37˚C in a humidified incubator (Thermo Fisher Scientific, Inc., Waltham, MA, USA), 5% CO_2, 95% air atmosphere. All of the experiments were performed after 48 h incubation with RPMI-1640 medium containing high glucose (HG, 30 mM D-glucose) or normal glucose (NG, 5 mM D-glucose). Human embryonic kidney (HEK) 293 T cells (American Type Culture Collection, ATCC, Manassas, USA) were incubated in Dulbecco's modified Eagle's medium (DMEM; Thermo Fisher Scientific, Inc.) and supplemented with 10% FBS, 100 μg/ml streptomycin and 100 IU/ml penicillin (all of them from Sigma-Aldrich, St. Louis, MO, USA). All of the experiments were repeated with at least three different cell preparations in triplicate.

ELISA assay. Total superoxide dismutase (SOD; cat. no: S0101) and malondialdehyde (MDA; cat. no: S0131) were determined using assay kits (Beyotime Institute of Biotechnology, Haimen, China), following the manufacturer's protocol.

ROS assay. The generation of ROS in the podocytes was evaluated using a fluorometry assay via the intracellular oxidation of dichlorodihydrofluorescein diacetate (DCFH-DA; Sigma-Aldrich). The cells ($4x10^5$) were incubated in a 6-well plate for 48 h, following DCFH-DA (50 μg/ml) incubation for 30 min at 37, the cells were harvested and washed with PBS 2 times and finally added into 1 ml PBS, which were detected and analyzed using flow cytometry (BD Biosciences, Franklin Lakes, NJ, USA). The fluorescent product 2',7'-dichlorofluorescein (DCF) was detected at an emission wavelength of 530 nm and excitation wavelength of 485 nm, and the result was analyzed using the flow cytometry analysis software BD CellQuest (v.5.1; Becton Dickinson, San Jose, CA, USA).

Caspase-3 activity assay. Podocytes ($1x10^6$) were lysated by NP-40 buffer, and the supernatant was collected for assay. In brief, 20 μl of cell lysate incubated with anti-caspase-3 antibody (cat. no: sc-7272; dilution, 1:200; Santa Cruz Biotechnology, Santa Cruz, CA, USA) at 37˚C for 1 h. The immunocomplexes were then incubated with peptide substrate (2 μl of 10 mM acetyl-Asp-Glu-Val-Asp-p-nitroanilide) in assay buffer (100 mM Hepes, pH 7.5, 20% v/v glycerol, 5 mM dithiothreitol, and 0.5 mM EDTA) for 2 h at 37˚C. The release of p-nitroaniline was measured at 405 nm using an ELISA reader (MD SpectraMax M5; Molecular Devices, LLC, Sunnyvale, CA, USA).

Transfection with miR-130a-3p and miR-301a-3p. The sequences of the miR-130-3p mimics (5'-CAGUGCAAU GUUAAAAGGGCAU-3'), mutant miR-130-3p (5'-CA**acaa c**AUGUUAAAAGGGCAU-3'), anti-miR-130-3p (antisense inhibitor of miR-130-3p: 5'-AUGCCCUUUUAACAUUGC ACUG-3'), mutant anti-miR-130-3p (5'-AUGCCCUUUUAA CAU**gaaca**UG-3'), miR-301a-3p mimics (5'-CAGUGCAAU AGUAUUGUCAAAGC-3'), mutant miR-301a-3p (5'-CA**acaa c**AUAGUAUUGUCAAAGC-3'), anti-miR-301a-3p (antisense inhibitor of miR-301a-3p: 5'-GCUUUGACAAUACUAUUG CACUG-3') and mutant anti-miR-301a-3p (5'-GCUUUG ACAAUACUAU**gaaca**UG-3') were synthesized by RiboBio (Guangzhou, China). The MPC5 podocytes were transfected using Lipofectamine 2000 (Invitrogen; Thermo Fisher Scientific, Inc.) at a final concentration of 50 nM. At 48 h post-transfection, the cells were harvested for analysis.

Dual-luciferase reporter gene assay. The potential binding site between miR-130a-3p/301a-3p and TNF-α was obtained using online predict software Targetscan (www.targetscan.org) and miRanda (www.microrna.org), and synthesized by RiboBio. The wild-type (WT) and mutant-type (MUT) 3'-UTR of TNF-α were inserted into the multiple cloning sites of the luciferase expressing pMIR-REPORT vector (Ambion; Thermo Fisher Scientific, Inc.). For the luciferase assay, the 293 T cells ($1x10^5$) were seeded into 24-wells and co-transfected with luciferase reporter vectors containing the WT and MUT of TNF-α-3'-UTR (0.5 μg) and mimics, antisense and corresponding mutant sequences of miR-130a-3p/301a-3p (50 nM) using Lipofectamine 2000 (Invitrogen; Thermo Fisher Scientific, Inc.). The luciferase activity was measured using a dual luciferase reporter assay kit (cat. no: RG027; Beyotime Institute of Biotechnology) according to the manufacturer's protocol.

Small interfering TNF-α (si-TNF-α) design and transfections. si-TNF-α (AGATTGAGGTGAAATCTTC) was designed using siDesigner (http://sidirect2.rnai.jp/) and synthesized by RiboBio. MPC5 podocytes were transfected with si-TNF-α and the scramble sequence, respectively. Moreover, cells were treated with TNF-α inhibitor (10 μM, cat. no: SAB4502989; Sigma-Aldrich), then the levels of ROS, SOD, MDA and caspase-3 and the protein expression of Bcl-2 and BAX were performed after 48 h treatment.

RNA analysis and Reverse transcription-quantitative polymerase chain reaction (RT-qPCR). Total RNA in podocyte was extracted by TRIzol (Invitrogen) according to the manufacturer's protocol. The cDNA was synthesized by reverse transcription reactions with 2 μg of total RNA using moloney murine leukemia virus reverse transcriptase (Invitrogen; Thermo Fisher Scientific, Inc.) according to the manufacturer's

protocol. PCR reaction mixtures were contained 12.5 μl SYBR Green Supermix (Bio-Rad Laboratories, Inc., Hercules, CA, USA), 1 μl cDNA, 300 nM of each primer, and DEPC H_2O to a final volume of 25 μl, and then RT-qPCR was performed using the Applied Biosystems 7300 Real-Time PCR System (Thermo Fisher Scientific, Inc.). The Cq (quantification cycle fluorescence value) was calculated using SDS software, version 2.1 (Applied Biosystems; Thermo Fisher Scientific, Inc.), and the relative expression levels of miRs and mRNA were calculated using the $2^{-\Delta\Delta Cq}$ method (22) and normalized to the internal control U6 and glyceraldehyde 3-phosphate dehydrogenase (GAPDH), respectively. The primers were synthesized by Sangon Biotech (Shanghai, China) as following: miR-130a-3p: Forward 5'-GCC CAGTGCAATGTTAAAAGGGCAT-3' and reverse 5'-CCA GTCTCAGGGTCCGAGGTATTC-3'; miR-301a-3p: Forward 5'-ACACTCCAGCTGGGCAGTGCAATAGTATTGTC-3' and reverse 5'-CTCAACTGGTGTCGTGGA-3'; U6: Forward 5'-CTCGCTTCGGCAGCACA-3' and reverse 5'-AACGCT TCACGAATTTGCGT-3'; TNF-α: Forward 5'-AAGCCCGTA GCCCACGTCGTA-3' and reverse 5'-GCCCGCAATCCAGGC CACTAC-3'; GAPDH: Forward 5'-GCACCGTCAAGCTGA GAAC-3' and reverse 5'-TGGTGAAGACGCCAGTGGA-3'.

Western blot analysis. Proteins were extracted with radio immunoprecipitation assay (RIPA) buffer (cat. no: P0013B; Beyotime Institute of Biotechnology) with protease inhibitors, and the concentrations were determined using the Bicinchoninic Acid Kit for Protein Determination (cat. no: BCA1-1KT; Sigma-Aldrich; Merck KGaA). 50 μg of protein for each sample was separated on a 10% SDS-PAGE gel and transferred to nitrocellulose membranes (Bio-Rad Laboratories, Inc.). After blocking with 5% non-fat dry milk at room temperature for 2 h, the membrances were incubated with the primary antibody of TNF-α (cat. no: sc-52746; dilution: 1:1,000), Bcl-2 (cat. no: sc-509; dilution: 1:1,000), BAX (cat. no: sc-70405; dilution: 1:1,000) and β-actin (cat. no: sc-130301; dilution: 1:2,000; all of them from Santa Cruz Biotechnology) at room temperature for 2 h. β-actin signals were used to correct for unequal loading. Following three washes with TBST, the membranes were incubated with the appropriate horseradish peroxidase-conjugated secondary antibody (cat. no: sc-516102; dilution: 1:10,000; Santa Cruz Biotechnology) at room temperature for 2 h and visualized by chemiluminescence (Thermo Fisher Scientific, Inc.). Signals were analyzed with Quantity One® software version 4.5 (Bio Rad Laboratories, Inc.).

Statistical analysis. Data were presented as the mean ± standard deviation (SD) for each group. All statistical analyses were performed using PRISM v5.0 (GraphPad Software, Inc., La Jolla, CA, USA). Inter-group differences were analyzed by one-way analysis of variance, followed by a post hoc Tukey test for multiple comparisons. $P<0.05$ was considered to indicate a statistically significant difference.

Results

HG induced the down-regulation of miR-130a-3p/301a-3p and the up-regulation of TNF-α in podocytes. Our preliminary analysis indicated that miR-130a-3p/301a-3p and TNF-α were closely related to HG-induced cell dysfunction. Thus, for the first steps we focused our experiments on the expression of miR-130a-3p/301a-3p and TNF-α in podocytes exposure to HG. The findings demonstrated that both miR-130a-3p and miR-301a-3p were significantly down-regulated in HG-incubated podocytes compared with control group (Fig. 1A). On the other hand, TNF-α was found robustly up-regualted in podocytes at both mRNA (Fig. 1B) and protein (Fig. 1C) levels in the present of HG. These results showed the deregulation of miR-130a-3p/301a-3p and TNF-α in HG condition.

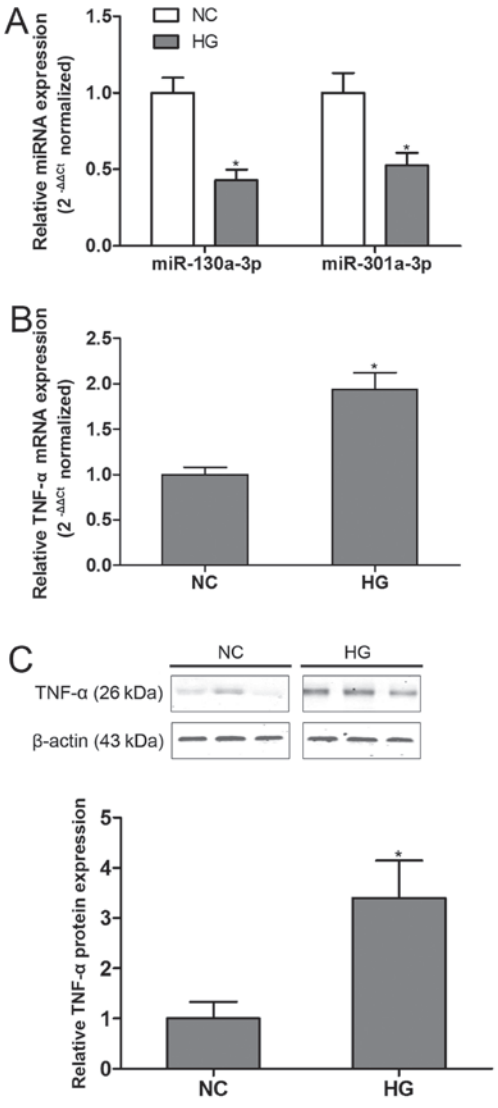

Figure 1. Reciprocal changes of miR-130a-3p/301a-3p and TNF-α expression in HG-incubated MPC5 podocytes. (A) The levels of miR-130a-3p and miR-301a-3p were performed by qRT-PCR after 48 h incubation with high glucose (HG, 30 mM D-glucose) or normal glucose (NG, 5 mM D-glucose). The mRNA (B) and protein (C) expression of TNF-α were measured by qRT-PCR and western blotting, respectively, after treatment with HG or NG for 48 h. n=3 in each group, *P<0.05 vs. NG group.

TNF-α was a direct target gene of miR-130a-3p/301a-3p. To investigate whether TNF-α was a direct target of miR-130a-3p/301a-3p, the online predict software Targetscan and miRanda were used for prediction. The results demonstrated that TNF-α was a direct target gene for both miR-130a-3p

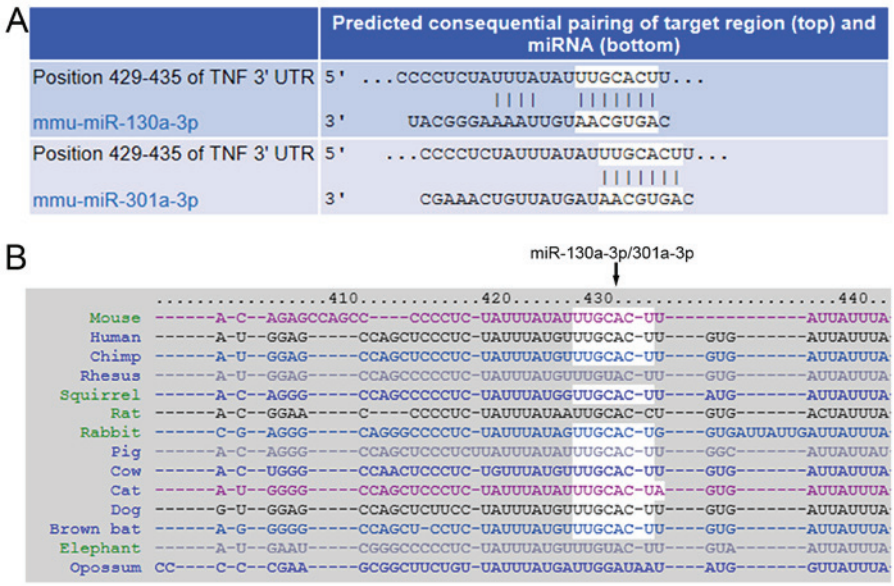

Figure 2. (A) Bioinformatics prediction of TNF-α as a candidate target gene for miR-130a-3p/301a-3p. Schematic representation of the putative miR-130a-3p/301a-3p binding site in the 3'UTR of TNF-α was predicted by the Targetscan and miRanda, and miR-130a-3p and miR-301a-3p shared the identical seed site of TNF-α. (B) The conserved sequence of binding sites between miR-130a-3p/301a-3p and TNF-α was shown across various species.

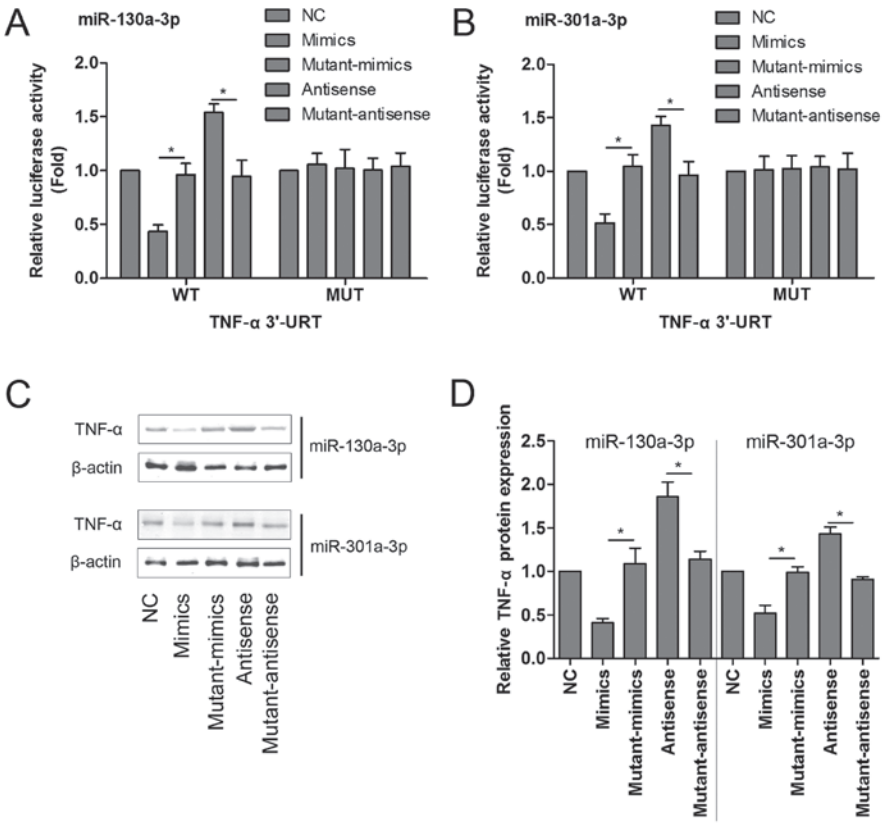

Figure 3. (A, B) TNF-α was a direct target gene of miR-130a-3p/301a-3p. The 293 T cells were co-transfected with the WT and MUT 3'-UTR of TNF-α and miR-130a-3p or miR-301a-3p mimics, antisense or corresponding mutation sequence, and the luciferase activity assay was performed after 48 h transfection. (C, D) The podocytes were transfected with miR-130a-3p or miR-301a-3p mimics, antisense or corresponding mutation sequence, the protein expression of TNF-α was measured by western blotting after 48 h transfection. n=3 in each group, $^{*}P<0.05$ vs. corresponding control group.

and miR-301a-3p that share the same 3'-UTR of target gene (Fig. 2A), which is highly conserved across species (Fig. 2B).

To confirm this, either the WT sequence of TNF-α or its mutant-type (MUT) sequence was transfected into the luciferase-reporter plasmids, and then the reporters were co-transfected with mimics, mutant-mimics, antisense or mutant-antisense of miR-130a-3p and miR-301a-3p into 293 T cells, and the levels of luciferase enzyme activity were

measured. As shown in Fig. 3A and B, transfection with miR-130a-3p or miR-301a-3p mimics significantly diminished the luciferase enzyme activity, but miR-130a-3p or miR-301a-3p antisense dramatically enhanced the luciferase activity in the presence of the WT 3'-UTR of TNF-α compared with corresponding control group. Mutant-mimics or mutant-antisense of miR-130a-3p and miR-301a-3p had no obvious affect on the luciferase enzyme activity.

To further determine whether TNF-α protein expression was regulated by miR-130a-3p or miR-301a-3p, the MPC5 podocytes were transfected with mimics, mutant-mimics, antisense or mutant-antisense of miR-130a-3p and miR-301a-3p, respectively, and the protein quantification assay of TNF-α was performed by western blotting. Our results showed that miR-130a-3p or miR-301a-3p mimics significantly reduced the protein expression of TNF-α. On the contrary, miR-130a-3p or miR-301a-3p antisense markedly increased TNF-α protein expression compared with corresponding control group (Fig. 3C and D).

Overexpressed miR-130a-3p/301a-3p inhibited HG-induced MPC5 podocytes dysfunction. Oxidative stress occurs when ROS affect the balance between oxidative pressure and antioxidant defense (23). SOD is an enzymatic scavenger of ROS, which can combat the accumulation of ROS and limit oxidative injury (24). In the present study, HG induced ROS generation, these change was partially reversed by miR-130a-3p or miR-301a-3p mimics transfection in MPC5 podocytes. Moreover, inhibition of miR-130a-3p or miR-301a-3p could significantly increased ROS generation as compared to corresponding control group (Fig. 4A). Intriguingly, exposure of podocytes to HG resulted in a remarkable reduction in SOD activity and a dramatic increase in MDA level, however, transfected with miR-130a-3p or miR-301a-3p mimics prevented these changes in podocytes (Fig. 4B and C). MDA is a lipid peroxidation product and is usually considered a reflection of cell injury (25). The present results showed that overexpressed miR-130a-3p or miR-301a-3p could ameliorate HG-induced MPC5 podocytes metabolic disturbance.

TNF-α loss-of-function alleviated HG-induced MPC5 podocytes dysfunction and apoptosis. We have shown that downregulation of miR-130a-3p/-301a-3p is accompanied by upregulation of TNF-α in HG-treated MPC5 podocytes. TNF-α is a cognate target for miR-130a-3p and miR-301a-3p. It is conceivable that TNF-α mediates HG-induced MPC5 podocytes dysfunction. TNF-α si-RNA was designed to confirm the hypothesis. We had confirmed that podocytes transfected with si-TNF-α or treated with TNF-α inhibitor could significantly reverse HG-induced the up-regulation of ROS (Fig. 5A). Moreover, si-TNF-α or TNF-α inhibitor prevented HG-induced a remarkable reduction in SOD activity and a dramatic increase in MDA levels in podocytes (Fig. 5B and C). Furthermore, TNF-α signaling in HG-induced podocytes apoptosis was investigated. We examined caspase-3 activity and Bcl-2 and BAX protein expression in podocytes with or without HG treatment. The results indicated that HG induced caspase-3 activation, however, podocytes transfected with si-TNF-α or treated with TNF-α inhibitor significantly inhibited caspase-3 activity (Fig. 5D). Exposure of podocytes

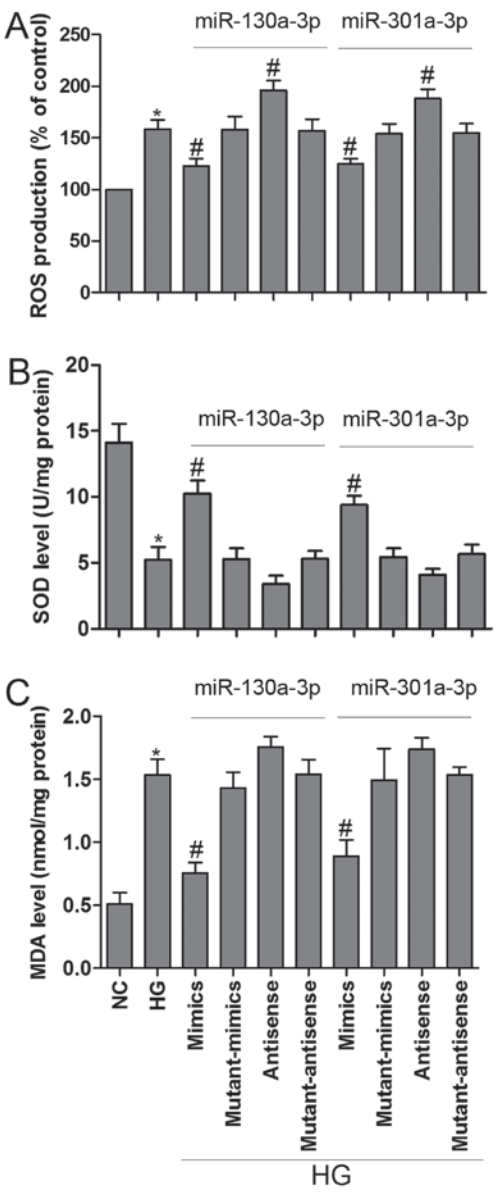

Figure 4. Overexpressed of miR-130a-3p and miR-301a-3p inhibited HG-induced ROS and oxidative stress in podocytes. The levels of (A) ROS, (B) SOD and (C) MDA were analyzed in podocytes with or without HG treatment, as well as transfected miR-130a-3p or miR-301a-3p mimics, antisense or corresponding mutation sequence. n = 3 in each group, $^{*}P<0.05$ vs. corresponding control group; $^{\#}P < 0.05$ vs. HG group.

to HG resulted in a significant decrease in Bcl-2 protein expression and Bcl-2/BAX ratio and a significant increase in BAX protein expression (Fig. 5E and F). Interestingly, podocytes transfected with si-TNF-α or treated with TNF-α inhibitor effectively reversed HG-induced the down-regulation of Bcl-2 protein expression and Bcl-2/BAX ratio and the up-regulation of BAX protein expression.

Discussion

This study demonstrated that miR-130a-3p/301a-3p was a novel regulator of TNF-α in mouse podocytes. Results of our bioinformatic analysis and luciferase reporter assay showed that miR-130a-3p/301a-3p directly interacted with the 3'-UTR of TNF-α. In MPC5 podocytes, the miR-130a-3p

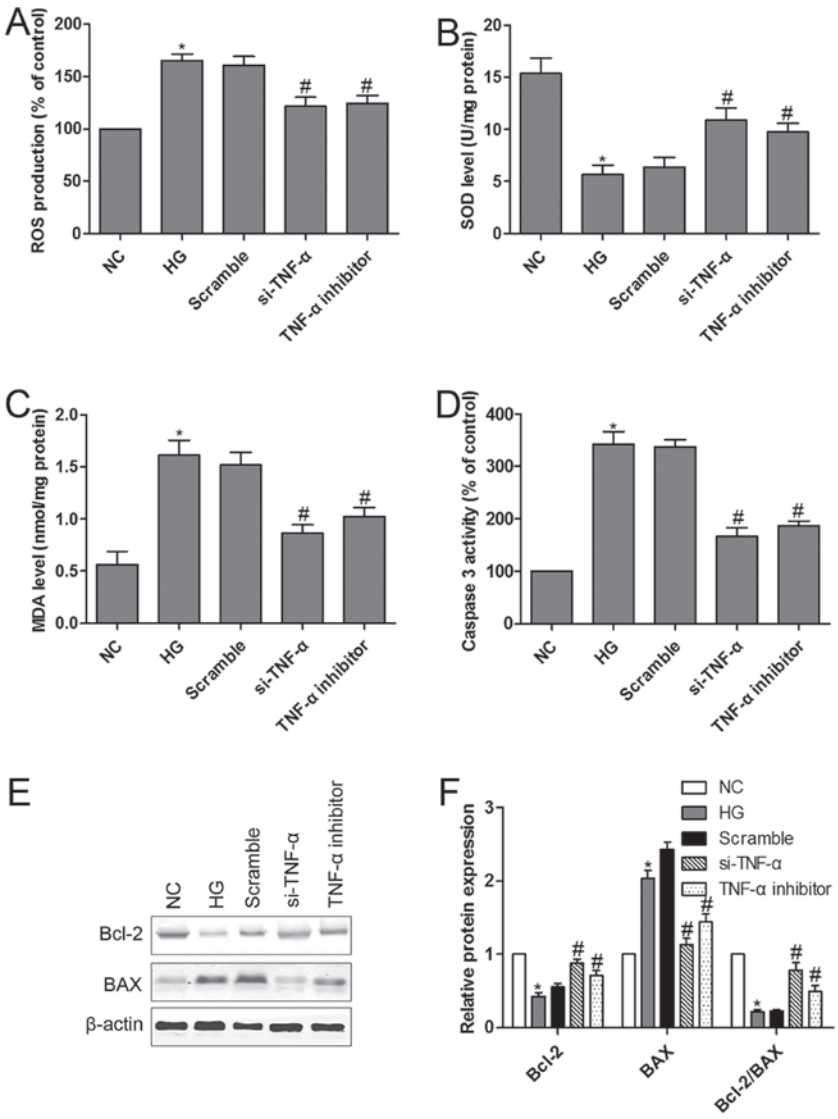

Figure 5. TNF-α loss-of-function alleviated HG-induced MPC5 podocytes dysfunction and apoptosis. The levels of (A) ROS, (B) SOD, (C) MDA and (D) caspase-3 were analyzed in podocytes with si-TNF-α transfection or TNF-α inhibitor treatment in the present or absence of HG. (E, F) The protein expression of Bcl-2 and BAX were measured by western blotting after 48 h treatment. n=3 in each group, *P<0.05 vs. NC group; #P<0.05 vs. HG group.

or miR-301a-3p mimic decreased the TNF-α protein expression, which was rescued by the miR-130a-3p or miR-301a-3p inhibitor. These results provide strong evidence that TNF-α was a direct target gene of miR-130a-3p/301a-3p. Here we showed forced expression of miR-130a-3p or miR-301a-3p via transfection of its mimic in cultured podocytes resulted in the down-regulation of ROS and MDA and the up-regulation of SOD in the present of HG. Moreover, inhibition of TNF-α level also prevented a remarkable reduction in SOD activity and a dramatic increase in ROS and MDA levels in HG-treated podocytes. The combined results above strongly suggested that overexpressed miR-130a-3p/301a-3p could significantly ameliorate HG-induced MPC5 podocytes dysfunction, and the underlying mechanism was mediated, at least partially, through the suppression of TNF-α expression.

In our study, we found that miR-130a-3p and miR-301a-3p shared the identical seed site of TNF-α. However, there has been no relevant report about the functional similarity between miR-130a-3p and miR-301a-3p in mammals. Our findings indicated that miR-130a-3p and miR-301a-3p had played a similar role in HG-induced MPC5 podocytes dysfunction. A recent study shows that miR-130a-3p is aberrantly reduced in livers of a mouse model with nonalcoholic fibrosing steatohepatitis, and the overexpression of miR-130a-3p inhibits hepatic stellate cells (HSC) activation and proliferation and promotes HSC apoptosis (26). Moreover, miR-130a-3p has been proven regulation of liver steatosis, glucose homeostasis and insulin sensitivity (10,21). miR-301a-3p, as an oncogene, has been reported to be upregulated in several malignant tumors (27,28). However, relatively little is known about the role of miR-301a-3p in HG-induced metabolic disorders. In our study, miR-130a-3p and miR-301a-3p collectively target to TNF-α inhibition of HG-induced podocytes dysfunction.

Inflammatory reaction is tightly regulated by altering TNF-α (29). Numerous studies have shown that TNF-α is implicated in the modulation of HG-induced cell dysfunction, including uterine epithelial cells, vascular smooth muscle cells (VSMCs) and primary human monocytes (30-32). We also found that TNF-α was upregulated in podocytes in the presence of HG, however, TNF-α loss-of-function blocked

HG-enhanced ROS and oxidative stress *in vitro*. Previous study has shown that podocytes may play a contributory role in the development of interstitial damage in IgA nephropathy by amplifying the activation of tubular epithelial cells with enhanced TNF-α synthesis after inflammatory changes of human mesangial cell (1). Serum levels of soluble TNF-α correlate with renal injury, and the possible mechanism shows that soluble TNF-α activates NF-κB and dose-dependently induces podocyte proliferation (33). Consistent with these reports, we also observed the correlation between the up-regulation of TNF-α expression and podocyte injury.

Numerous studies have shown that TNF-α is a potential therapeutic target for chronic kidney disease (CKD) and glomerulonephritis (34,35). Our data confirmed that TNF-α was a target gene of miR-130a-3p and miR-301a-3p. We also observed an inhibitory effect of si-TNF-α on HG-induced oxidative stress and apoposis in podocytes, which could increase intrarenal renin-angiotensin system (RAS) activity and reduce nitric oxide (NO) availability to trigger glomerular disease (36). Because TNF-α is involved in HG-induced podocytes dysfunction, our results suggest that miR-130a-3p or miR-301a-3p is likely to be a novel biomarker or new potent therapeutic target for podocytes injury-related renal disease.

Taken together, the data obtained in our study support the conclusion that miR-130a-3p/301a-3p targeting to TNF-α inhibits HG-induced oxidative stress and apoposis in podocytes, and suggest that a novel function for miR-130a-3p/301a-3p in podocytes injury-related renal disease. Our results are also important in providing new perspective for the understanding of the underlying molecular mechanisms in podocytes dysfunction and potential therapeutic target for glomerulonephritis.

Acknowledgements

This work was supported by the United Fund of the Department of Science and Technology in Guizhou Province of China (Grant no: LH-2016-7395).

References

1. Lai KN, Leung JC, Chan LY, Saleem MA, Mathieson PW, Lai FM and Tang SC: Activation of podocytes by mesangial-derived TNF-alpha: Glomerulo-podocytic communication in IgA nephropathy. Am J Physiol Renal Physiol 294: F945-F955, 2008.
2. D'Amico G and Bazzi C: Pathophysiology of proteinuria. Kidney Int 63: 809-825, 2003.
3. Huang G, Zou B, Lv J, Li T, Huai G, Xiang S, Lu S, Luo H, Zhang Y, Jin Y and Wang Y: Notoginsenoside R1 attenuates glucose-induced podocyte injury via the inhibition of apoptosis and the activation of autophagy through the PI3K/Akt/mTOR signaling pathway. Int J Mol Med 39: 559-568, 2017.
4. Verzola D, Gandolfo MT, Ferrario F, Rastaldi MP, Villaggio B, Gianiorio F, Giannoni M, Rimoldi L, Lauria F, Miji M, *et al*: Apoptosis in the kidneys of patients with type II diabetic nephropathy. Kidney Int 72: 1262-1272, 2007.
5. White KE, Bilous RW, Marshall SM, El Nahas M, Remuzzi G, Piras G, De Cosmo S and Viberti G: Podocyte number in normotensive type 1 diabetic patients with albuminuria. Diabetes 51: 3083-3089, 2002.
6. Yang H, Wang Q and Li S: MicroRNA-218 promotes high glucose-induced apoptosis in podocytes by targeting heme oxygenase-1. Biochem Biophys Res Commun 471: 582-588, 2016.
7. Dai H, Zhang Y, Yuan L, Wu J, Ma L and Shi H: CTGF mediates high-glucose induced epithelial-mesenchymal transition through activation of β-catenin in podocytes. Ren Fail 38: 1711-1716, 2016.
8. Jin Y, Liu S, Ma Q, Xiao D and Chen L: Berberine enhances the AMPK activation and autophagy and mitigates high glucose-induced apoptosis of mouse podocytes. Eur J Pharmacol 794: 106-114, 2017.
9. Ma L, Han C, Peng T, Li N, Zhang B, Zhen X and Yang X: Ang-(1-7) inhibited mitochondrial fission in high-glucose-induced podocytes by upregulation of miR-30a and downregulation of Drp1 and p53. J Chin Med Assoc 79: 597-604, 2016.
10. Xiao F, Yu J, Liu B, Guo Y, Li K, Deng J, Zhang J, Wang C, Chen S, Du Y, *et al*: A novel function of microRNA 130a-3p in hepatic insulin sensitivity and liver steatosis. Diabetes 63: 2631-2642, 2014.
11. Ofori JK, Salunkhe VA, Bagge A, Vishnu N, Nagao M, Mulder H, Wollheim CB, Eliasson L and Esguerra JL: Elevated miR-130a/miR130b/miR-152 expression reduces intracellular ATP levels in the pancreatic beta cell. Sci Rep 7: 44986, 2017.
12. Samandari N, Mirza AH, Nielsen LB, Kaur S, Hougaard P, Fredheim S, Mortensen HB and Pociot F: Circulating microRNA levels predict residual beta cell function and glycaemic control in children with type 1 diabetes mellitus. Diabetologia 60: 354-363, 2017.
13. Panguluri SK, Tur J, Chapalamadugu KC, Katnik C, Cuevas J and Tipparaju SM: MicroRNA-301a mediated regulation of Kv4.2 in diabetes: Identification of key modulators. PLoS One 8: e60545, 2013.
14. Zhou Z, Wan J, Hou X, Geng J, Li X and Bai X: MicroRNA-27a promotes podocyte injury via PPARγ-mediated β-catenin activation in diabetic nephropathy. Cell Death Dis 8: e2658, 2017.
15. Zhang X, Song S and Luo H: Regulation of podocyte lesions in diabetic nephropathy via miR-34a in the Notch signaling pathway. Medicine 95: e5050, 2016.
16. Chen YQ, Wang XX, Yao XM, Zhang DL, Yang XF, Tian SF and Wang NS: MicroRNA-195 promotes apoptosis in mouse podocytes via enhanced caspase activity driven by BCL2 insufficiency. Am J Nephrol 34: 549-559, 2011.
17. Sun J, Li ZP, Zhang RQ and Zhang HM: Repression of miR-217 protects against high glucose-induced podocyte injury and insulin resistance by restoring PTEN-mediated autophagy pathway. Biochem Biophys Res Commun 483: 318-324, 2017.
18. Lin CL, Lee PH, Hsu YC, Ko JY, Chuang PC, Huang YT, Wang SY, Wu SL, Chen YS, Chiang WC, *et al*: MicroRNA-29a promotion of nephrin acetylation ameliorates hyperglycemia-induced podocyte dysfunction. J Am Soc Nephrol 25: 1698-1709, 2014.
19. Lagos-Quintana M, Rauhut R, Yalcin A, Meyer J, Lendeckel W and Tuschl T: Identification of tissue-specific microRNAs from mouse. Curr Biol 12: 735-739, 2002.
20. Hosako H, Martin GS, Barrier M, Chen YA, Ivanov IV and Mirkes PE: Gene and microRNA expression in p53-deficient day 8.5 mouse embryos. Birth Defects Res A Clin Mol Teratol 85: 546-555, 2009.
21. Esguerra JL, Bolmeson C, Cilio CM and Eliasson L: Differential glucose-regulation of microRNAs in pancreatic islets of non-obese type 2 diabetes model Goto-Kakizaki rat. PLoS One 6: e18613, 2011.
22. Livak KJ and Schmittgen TD: Analysis of relative gene expression data using real-time quantitative PCR and the 2(-Delta Delta C(T)) method. Methods 25: 402-408, 2001.
23. Sun LN, Liu XC, Chen XJ, Guan GJ and Liu G: Curcumin attenuates high glucose-induced podocyte apoptosis by regulating functional connections between caveolin-1 phosphorylation and ROS. Acta Pharmacol Sin 37: 645-655, 2016.
24. Sun WH, Liu F, Chen Y and Zhu YC: Hydrogen sulfide decreases the levels of ROS by inhibiting mitochondrial complex IV and increasing SOD activities in cardiomyocytes under ischemia/reperfusion. Biochem Biophys Res Commun 421: 164-169, 2012.
25. Rahman MM, Muse AY, Khan DMIO, Ahmed IH, Subhan N, Reza HM, Alam MA, Nahar L and Sarker SD: Apocynin prevented inflammation and oxidative stress in carbon tetra chloride induced hepatic dysfunction in rats. Biomed Pharmacother 92: 421-428, 2017.
26. Wang Y, Du J, Niu X, Fu N, Wang R, Zhang Y, Zhao S, Sun D and Nan Y: MiR-130a-3p attenuates activation and induces apoptosis of hepatic stellate cells in nonalcoholic fibrosing steatohepatitis by directly targeting TGFBR1 and TGFBR2. Cell Death Dis 8: e2792, 2017.
27. Lu Y, Gao W, Zhang C, Wen S, Huangfu H, Kang J and Wang B: Hsa-miR-301a-3p acts as an oncogene in laryngeal squamous cell carcinoma via target regulation of Smad4. J Cancer 6: 1260-1275, 2015.

28. Xia X, Zhang K, Cen G, Jiang T, Cao J, Huang K, Huang C, Zhao Q and Qiu Z: MicroRNA-301a-3p promotes pancreatic cancer progression via negative regulation of SMAD4. Oncotarget 6: 21046-21063, 2015.
29. West NR, Hegazy AN, Owens BMJ, Bullers SJ, Linggi B, Buonocore S, Coccia M, Görtz D, This S, Stockenhuber K, *et al*: Oncostatin M drives intestinal inflammation and predicts response to tumor necrosis factor-neutralizing therapy in patients with inflammatory bowel disease. Nat Med 23: 579-589, 2017.
30. Pampfer S, Cordi S, Dutrieux C, Vanderheyden I, Marchand C and De Hertogh R: Interleukin 1beta mediates the effect of high D-glucose on the secretion of TNF-alpha by mouse uterine epithelial cells. Cytokine 11: 500-509, 1999.
31. Reddy AB, Ramana KV, Srivastava S, Bhatnagar A and Srivastava SK: Aldose reductase regulates high glucose-induced ectodomain shedding of tumor necrosis factor (TNF)-alpha via protein kinase C-delta and TNF-alpha converting enzyme in vascular smooth muscle cells. Endocrinology 150: 63-74, 2009.
32. Gonzalez Y, Herrera MT, Soldevila G, Garcia-Garcia L, Fabián G, Pérez-Armendariz EM, Bobadilla K, Guzmán-Beltrán S, Sada E and Torres M: High glucose concentrations induce TNF-α production through the down-regulation of CD33 in primary human monocytes. BMC Immunol 13: 19, 2012.
33. Bruggeman LA, Drawz PE, Kahoud N, Lin K, Barisoni L and Nelson PJ: TNFR2 interposes the proliferative and NF-κB-mediated inflammatory response by podocytes to TNF-α. Lab Invest 91: 413-425, 2011.
34. Khan SB, Cook HT, Bhangal G, Smith J, Tam FW and Pusey CD: Antibody blockade of TNF-alpha reduces inflammation and scarring in experimental crescentic glomerulonephritis. Kidney Int 67: 1812-1820, 2005.
35. Basturk T, Unsal A, Ulas T, Koc Y, Sakaci T, Ahbap E and Borlu F: Effects of rosiglitazone treatment on insulin resistance and TNF-alpha levels in patients with chronic kidney disease: A prospective study. Eur Rev Med Pharmacol Sci 16: 1519-1524, 2012.
36. Camici M, Carpi A, Cini G, Galetta F and Abraham N: Podocyte dysfunction in aging-related glomerulosclerosis. Front Biosci (Schol Ed) 3: 995-1006, 2011.